Journal of Imaging Science and Technology® 52(2): 020604–020604-9, 2008.

Multi-Ink Color-Separation Algorithm Improving Image Quality

Yongda Chen, Roy S. Berns, Lawrence A. Taplin and Francisco H. Imai
Munsell Color Science Laboratory, Chester F. Carlson Center for Imaging Science,
Rochester Institute of Technology, Rochester, NY 14623
E-mail: yxc6352@cis.rit.edu

Abstract. *Current color-printing technologies often use more than the minimum three or four inks: cyan, magenta, yellow, and black (CMYK). When the number of inks exceeds three, there is the usual color-management one-to-many mapping problem. Additional constraints have to be applied to achieve greater determinacy. For CMYK ink sets, the black ink is constrained. When additional chromatic inks are added, traditional methods subdivide either colorimetric or colorant space to achieve a one-to-one mapping. However, these traditional methods cannot take advantage of all the ink combinations available for improving image quality. Alternatively, additional constraints can be defined as perceptual metrics such as color constancy, graininess, color gamut, and color look-up table smoothness. A novel color separation algorithm was developed in order to optimize color look-up tables for improved image quality. This algorithm was tested with a six-pigmented ink (CMYKGO), ink jet proofing printer. Various four and a six-ink look-up tables were created based on different metrics. The perceptual performances of these look-up tables in color reproduction accuracy, color inconstancy, graininess and gamut volume were evaluated. The results show that the additional inks not only extend color gamut but also provided the potential to improve print quality. © 2008 Society for Imaging Science and Technology.*
[DOI: 10.2352/J.ImagingSci.Technol.(2008)52:2(020604)]

INTRODUCTION

As digital color printing demands continue to grow, there is a continuing need for color characterization. For a three-ink Cyan, Magenta, and Yellow (CMY) printer, the mapping from ink amounts to colorimetric coordinates is unique and various interpolations or fitting techniques can be applied directly. For a four-ink CMYK printer where K represents black, redundancy is introduced with the addition of the black ink. Generally one specific color can be produced by one CMY ink combination, whereas many CMYK ink combinations, depending on the black ink amount, may suffice. The inverse characterization for a CMYK ink set is generally performed by various methods of controlling the black ink amount. These methods include black addition, under-color removal (UCR), or gray-component replacement (GCR), which are traceable to the graphic arts printing industry.[1]

For high-fidelity color printing—printing with additional chromatic inks—the color gamut is extended, but considerable redundancy is introduced into the color reproduction process in that many ink combinations can produce the same color and even the same spectra.[2] In order to create a one-to-one color look-up table, additional constraints are needed to improve determinacy for multi-ink printing. One strategy is to separate the color gamut into sub-gamuts. Kueppers[3] and Ostromoukhov[4] separated the color gamut into sub-gamuts formed by three-ink combinations. For example, Red, Green, and Blue inks were added to create a CMYKRGB ink set. Its color gamut was separated into six sub-gamuts produced by the ink combinations: CGK, GYK, YRK, RMK, MBK, and BCK. Balasubramanian[5] partitioned the gamut into sub-gamuts produced by four-ink combinations, and UCR or GCR was employed to produce color separations as in CMYK printing. Boll[6] also separated the gamut into sub-gamuts produced by four-colorant combinations, and a unique one-to-one mapping was created by adding constraints such as minimizing area coverage and smoothing the transitions between sub-gamuts. Dalal[7] separated the whole gamut into the sub-gamut formed from the traditional CMYK ink combinations and the sub-gamut extended by additional inks, which were only used to reproduce colors outside of the traditional CMYK sub-gamut.

A color gamut partition strategy can guarantee the one-to-one relationship between colorimetric values and ink combinations and constrains the number of possible ink combinations. However, various ink combinations have different colorimetric and spatial properties in prints. The additional inks cannot only extend the color gamut but also provide the potential to improve perceptual image quality such as color constancy and graininess. The traditional methods cannot fully realize this potential to improve image quality and even lose part of color gamut without utilizing the full range of ink combinations.

In this research, a new color separation method was developed in which perceptual metrics were used to choose samples for the construction of look-up tables from candidate ink combinations that have similar CIELAB values. These perceptual metrics include color inconstancy, graininess, chroma, and color look-up table smoothness.

Color inconstancy is a very important factor to evaluate the image quality of prints since prints are viewed under many different lighting conditions. For example, color inconstancy occurs frequently when profiles are created for standardized daylight (D50) but viewed under narrowband

Received Feb. 20, 2007; accepted for publication Nov. 26, 2007; published online Apr. 2, 2008.
1062-3701/2008/52(2)/020604/9/$20.00.

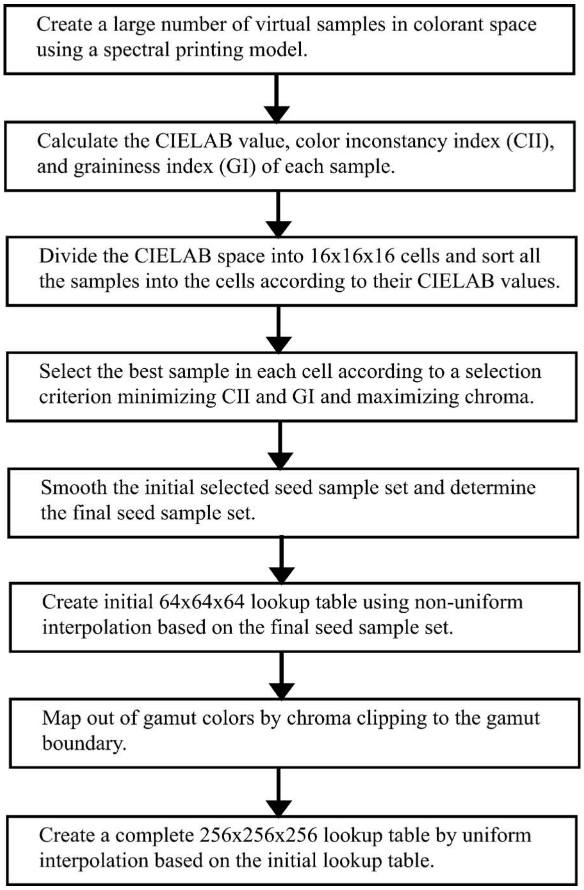

Figure 1. Flowchart of creating color look-up table for multiple-ink printers.

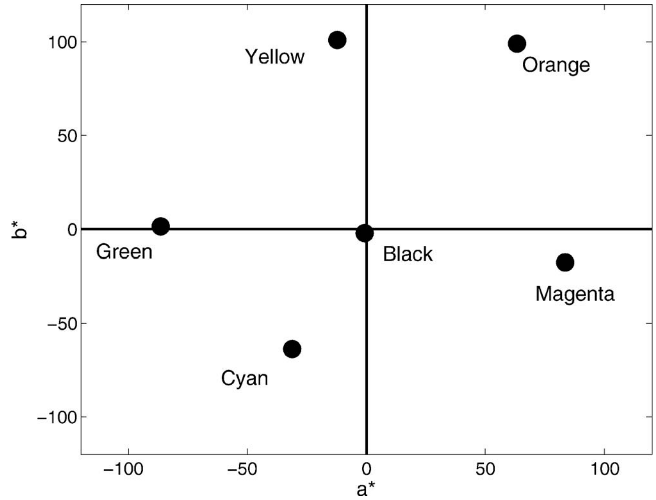

Figure 2. CMYKGO ink positions projected onto the a*b* plane.

fluorescent illumination (F11). Another factor resulting in poor quality is image noise. One of the most important, well-known categories of image noise is graininess, a subjective impression of spatial non-uniformity in an image. Gamut volume is always desirable for color reproduction and look-up tables should take full advantage of the maximum color gamut achievable by the set of inks and a specific substrate.

Smoothness, the similarity of ink combinations among adjacent nodes in a look-up table, is also a very important factor and can affect interpolation accuracy. Though different ink combinations with different spectra show similar perceptual colors under a specific illuminant, they may shift in different perceptual directions when the illuminant is changed causing a color-uniform image to become non-uniform.

The proposed algorithm will use these perceptual metrics to choose seed samples that are used to create final look-up tables producing prints with high image quality.

ALGORITHM OVERVIEW

The goal of this algorithm was to optimize a color look-up table (CLUT) that converted CIELAB to multiple ink separations for print quality. Figure 1 illustrates the proposed algorithm's flowchart. First, a spectral printing model was developed to predict the spectral reflectance of prints, required to compute a color inconstancy metric and CIELAB values. Using this model, a large number of virtual samples was created in a multiple colorant space, and their tristimulus values calculated for a specific illuminant and a single standard observer. The sampling goal was to have a sufficient number of virtual samples such that in every region of the color gamut defined in CIELAB for D50, there were multiple ink combinations. Then, CIELAB space was divided into coarsely sampled cells, and the samples binned into these cells. For each cell, a specific metric was used to select a seed sample. The sample selection criteria included color reproduction qualities such as color gamut and color constancy, and spatial image quality such as graininess. Based on the initial seed sample set, a smoothness metric was added to determine the final seed sample set. Next, non-uniform interpolation was used to populate a finer sampled grid ($64\times64\times64$) from the final seed sample set. Although additional inks extended color gamut significantly, many perceived colors are still outside of the printable gamut. Gamut mapping is always necessary to populate the CLUT with area coverages for out-of-gamut colors. In this research, a simple method, chroma clipping, was used: C^*_{ab} clipping maintaining h_{ab} and L^* for colors within the L^* range of the printer. Colors darker or lighter than the printer gamut were mapped to the darkest and lightest neutral ($a^*=b^*=0$). Finally the $64\times64\times64$ grid was extended to a fully populated $256\times256\times256$ color look-up table (CLUT) by linear interpolation in order to improve processing speed for color separating images and to eliminate CLUT size as a source of error.

Multiple-Ink Printer and its Spectral Printing Model

An Epson Pro 5500 ink jet printer was used in this research. This was a six-ink printer normally equipped with cyan, magenta, yellow, black, light cyan, and light magenta pigmented inks. The light cyan and magenta were replaced with green and orange—a CMYKGO ink set. Their positions in the a^*b^* projection are shown in Figure 2. Software was provided by the manufacturer that enabled direct access to each

Table I. Accuracy of the printing model.

Spectral RMS error		ΔE_{00}		MI under D50		MI under A	
Mean	Max	Mean	Max	Mean	Max	Mean	Max
0.5%	2.6%	1.0	3.3	0.2	1.0	0.2	1.2

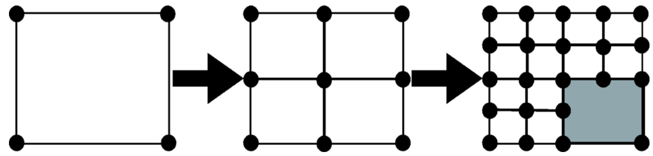

Figure 3. A demonstration of two-dimensional quad-tree decomposition.

colorant as a six-dimensional 8 bit per color plane image file; that is, it bypassed any embedded color management. The halftoning algorithm was proprietary and not made available. Typical of commercial ink jet printers, the algorithm was very complex where there were interactions between color planes. That is, halftoning was not a single pixel-wise process repeated six times for each color plane.

The cellular Yule-Nielsen modified spectral Neugebauer model (CYNSN) was first created,[8] in similar fashion to Taplin and Berns.[9] This model is an additive-mixing model where each printed color type positioned at the vertices of each cell, defined as $R^{1/n}_{\lambda,Cellular\ Primary}$, is weight averaged, the weighting dependent on the halftoning algorithm. For this printer, its halftoning was treated as a random process (i.e., defined using the DeMichel equations). There were two reasons for subdividing the colorant space into cells. First, the complex halftoning was better approximated as a random process when the colorant space was limited in volume. Second, limitations in the additive mixing model caused by approximating the ink and paper optics via $R^{1/n}_{\lambda}$ was minimized by increasing the number of measured colors. Three optimizations were performed to find the optimal Yule–Nielsen n value, the optimal positions of the four cellular primaries for each ink, and the optimal spectral estimation of non-printable ink combinations due to maximum ink limitations. A target composed of 600 randomly generated colors in colorant space was printed and measured spectrally. The accuracy of the printer model was evaluated by comparing these measured spectra and derived CIELAB values with the printer model predictions, shown in Table I. The mean and maximum color differences (D50, 2° observer) were 1.0 and 3.3 ΔE_{00}, respectively, and the mean and maximum RMS spectral errors were 0.5% and 2.6%, respectively. A metameric index[10] (MI) under D50 was calculated after the predicted spectrum was paramerically corrected[11] to perfectly match the measured spectrum for illuminant A, and vice-versa for the MI under A. This index has units of ΔE_{00}. According to the evaluation data in Table I, this CYNSN printer model achieved sufficient accuracy for building color profiles.

Creation of Virtual Sample Set

The first phase of the proposed algorithm was to create a virtual sample set of ink combinations that sufficiently spanned CIELAB space and, whenever possible, provided different ink combinations with similar colorimetry. Originally, the virtual samples were created by combining area coverages of different inks from 0% to 100% in 10% intervals for each ink.[12] This simplistic method resulted in a high proportion of dark samples and a non-uniform distribution of samples in CIELAB space, both adversely affecting the quality of the final color look-up table. For example, if missed ink combinations were the best choices according to the selection metric, the smoothness of the look-up table and print quality would be affected.

After testing several methods and comparing computation time and computation load, a method called six-dimensional, quad-tree decomposition was adopted. This method worked by dividing the colorant space into equal-sized square blocks, and then testing the CIELAB differences among vertices of each block to see if they met a threshold criterion. If the criterion was met, the block was not further divided. If not, it was subdivided again into smaller blocks and new vertices were added, and the test criterion was applied to those blocks. This process was repeated iteratively until each block met the criterion.

First, 64 vertices in the six-dimensional, colorant space were chosen as the initial data set where each vertical had ink amounts of 0 or 1. Next, adjacent pairs of vertices were found. For example, if ink amounts are described as a vector $[c\ m\ y\ k\ g\ o]'$, then an adjacent pair is described as $[0\ 0\ 0\ 0\ 0\ 0]'$ and $[1\ 0\ 0\ 0\ 0\ 0]'$. The distance in CIELAB space between the adjacent pairs was calculated and if larger than a specific threshold, the midpoint of the adjacent point pair was added into the data set. According to this example, the sample $[0.5\ 0\ 0\ 0\ 0\ 0]'$ would be inserted. This process continued until the virtual sample set sufficiently covered CIELAB space. The threshold of distance between an adjacent pair of samples was selected based on data processing capability of the computer. Small thresholds create more samples, but at the expense of extremely slow processing speeds or system failure. For this research, the threshold was 2.5 ΔE^*_{ab}, a value that was a compromise between the number of generated samples and processing capabilities.

For the purpose of illustration, a two-dimensional quad-tree decomposition method is shown in Figure 3. If the distances in CIELAB space between these adjacent pairs are less than the threshold, no new point is added as shown as gray in Fig. 3. With this method, a reasonable database for the virtual sample dataset was created and distributed uniformly in CIELAB space.

Using this method plus adding samples to fill the edge of the color gamut, 1,123,454 samples were created and their tristimulus values calculated for Illuminant D50. The tristimulus values of the substrate were used as the white point in the CIELAB calculations to generate a CLUT with relative colorimetric rendering intent resulting in an expanded gamut compared with the approach using an absolute D50 white point. Figure 4 shows the lightness distribution of the new samples that are close to a normal

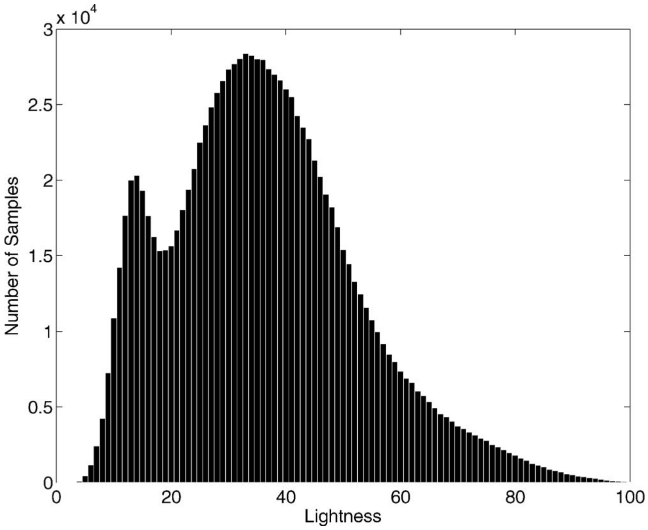

Figure 4. Histogram of CIE lightness of virtual sample set.

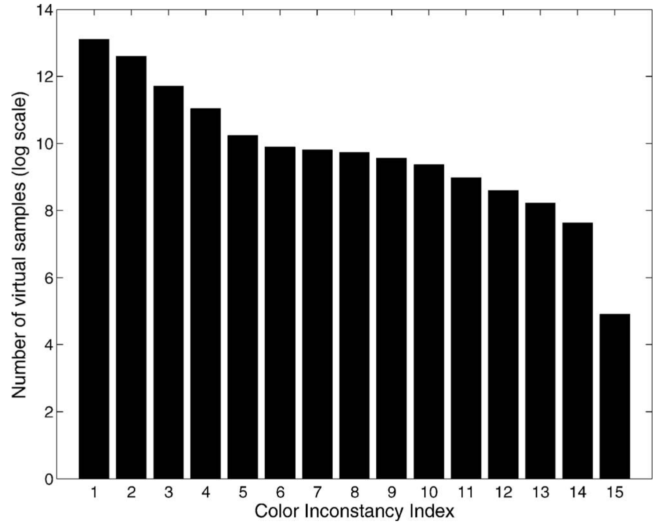

Figure 5. Color inconstancy index (CII) histogram of the virtual sample set (note logarithmic scale).

distribution—the first maximum occurring because of extra samples in order to fill the gamut boundary completely.

Perceptual Metrics

The perceptual metrics used in this algorithm to select the seed sample set included color constancy, graininess, color gamut, and smoothness. Color constancy is the general tendency of the color of an object to remain constant when the level and color of the illumination are changed.[11] It is a result of both physiological and psychological compensations. There does not yet exist a computational theory sufficient to explain the mechanism of the color constancy of human vision. Conversely, color inconstancy is the undesirable change in color caused by changes in illumination.

An index of color inconstancy, Color Inconstancy Index (CII), was used to evaluate the color variation under different illuminants, and its calculation was similar to those described in Refs. 10, 13, and 14. Tristimulus values were calculated for the test illuminant and the reference illuminant from the predicted spectral reflectance. Using the chromatic-adaptation transform from the CIECAM02 color-appearance model,[15] corresponding colors were calculated from each illuminant to D65. The corresponding tristimulus values were converted to CIELAB using D65 as the reference white. A weighted CIE94 color difference was then calculated between pairs of corresponding colors where hue inconstancy was penalized twice as much as lightness or chroma inconstancy, as shown in following equation.

$$CII = \left[\left(\frac{\Delta L^*}{2S_L} \right)^2 + \left(\frac{\Delta C^*_{ab}}{2S_c} \right)^2 + \left(\frac{\Delta H^*_{ab}}{S_H} \right)^2 \right]^{1/2}, \quad (1)$$

where

$$\Delta L^* = L^*_{\text{refer\_}c} - L^*_{\text{test\_}c}$$

$$\Delta C^*_{ab} = C^*_{\text{refer\_}c} - C^*_{\text{test\_}c}$$

$$\Delta H^*_{ab} = [(\Delta E^*)^2 - (\Delta L^*)^2 - (\Delta C^*)^2]^{1/2}$$

$$\Delta E^* = [(\Delta L^*)^2 + (\Delta a^*)^2 + (\Delta b^*)^2]^{1/2}$$

$$S_L = 1$$

$$S_C = 1 + 0.045 C^*_{\text{refer,test}}$$

$$S_H = 1 + 0.015 C^*_{\text{refer,test}}$$

$$C^*_{\text{refer,test}} = \sqrt{C^*_{\text{refer\_}c} \cdot C^*_{\text{test\_}c}},$$

where ΔC^*_{ab} represents the difference of chroma, ΔH^*_{ab} represents the difference of hue, and subscripts *refer* and *test* define reference and test illuminants, respectively.

In this research, the CII was calculated for CIE illuminant F11 (narrowband fluorescent) as the test illuminant compared with D50 as the reference illuminant. A CII histogram of the virtual sample set is shown in Figure 5. Many ink combinations have appreciable color inconstancy. As a rule of thumb, samples with excellent color constancy have CII values below unity.

Graininess was another image quality metric used to select seed samples. For halftone imaging, graininess arises in part from variations in the shape, size, edge roughness, and the scattered ink between the individual halftone dots. Graininess is greatest for images at low area coverages where halftone dots are isolated and have high contrast compared with the paper substrate. Many of the physical processes that give rise to these variations are uncorrelated from dot to dot. This lack of correlation will lead to a frequency-independent noise power spectrum. Several methods[16,17] to evaluate graininess objectively have been proposed with *a priori* knowledge of the halftone algorithm. In this research, the halftoning algorithm was unknown. As a consequence, prints sampling the colorant space were scanned and an empirical model was developed to predict image statistics from the six image planes.

Zhang[18] described a model that extended the standard CIELAB ΔE^*_{ab} equation, known as the S-CIELAB metric, to determine perceived differences in color images. The S-CIELAB metric was originally designed to measure color reproduction error using the spatial extension of CIELAB. In this research, a modified S-CIELAB metric suggested by Johnson[19] was used to measure the uniformity of halftone prints. RGB image scans were transformed into an opponent-colors space, AC_1C_2, and a spatial filtering operation applied to simulate spatial blurring by the human visual system. The average CIEDE2000 color difference was then calculated as a Graininess Index, GI, from the mean CIELAB value of the original color patch transformed from the scanned RGB values by device characterization and CIELAB values in the blurred color patch, as shown in the following equation:

$$\mathrm{GI} = \frac{\sum_{pixel=1}^{n}(CIEDE2000(Lab_{\mathrm{blured,pixel}}, Lab_{\mathrm{mean}}))}{n}. \quad (2)$$

An Epson Perfection 2450 Photo scanner was used to scan the prints at its maximum optical resolution of 2400 pixels per inch (ppi). However, we did not characterize and account for its spatial image quality and as a consequence, creating spatially filtered images as a function of cycles per degree of visual angle based on specific viewing distances and the printer addressability did not well predict visual inspection. As a consequence, images were calculated for a range of viewing distances between 3 and 18 in. and viewed on a high-resolution LCD display at a typical viewing distance. It was found that the viewing distance of 5 in., corresponding to 212 cycle per degree of visual angle, generated appropriate images for the graininess calculation.

For each ink, color ramps were printed and the GI calculated for each patch. As expected, the black ink patches resulted in much higher graininess than the other color ramps; the black ink had the lowest luminance factor (highest density) of the six inks and when compared with the white substrate, resulted in the largest luminance contrast, the dominant contributor to graininess. Conversely, the yellow ink had the highest luminance factor (lowest density) resulting in low luminance contrast compared with the substrate, and as a consequence, low graininess. The graininess indices for the black and yellow ramps are shown in Figure 6. The extreme graininess indices are caused by impurities on the target and scanner even though they were cleaned several times. Detector noise also contributed to these extrema. For the black ink, graininess was most evident in the midtones where the slope was constant. Hence, the print medium has maximum contrast, and the eye can more readily distinguish small luminance factor differences.

Because of the halftoning complexity, it was not possible to create an effective model that predicted graininess from digital signals. Instead, a cellular approach was used where

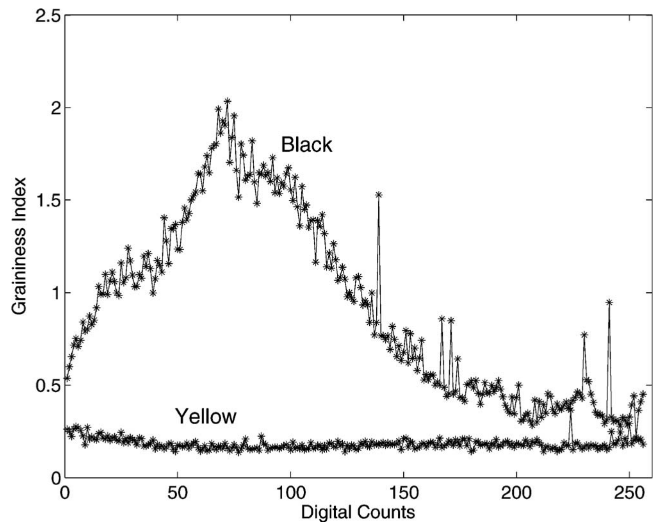

Figure 6. Graininess Index for black and yellow ramps.

within the cell, the average graininess was used. The six-dimensional colorant space was divided into small cells corresponding to four levels of area coverage: none, a little, most, and full. The mean graininess for all samples in each cell was then calculated representing the graininess of all ink combinations in the cell. Although this statistical model could not predict the graininess for each individual ink combination accurately, it did decrease prediction noise and provided an average graininess index for a group of adjacent samples in the colorant space. Because the purpose of this research was to develop a color separation algorithm that optimized image quality attributes, the precise models for the criteria of print quality, such as graininess and smoothness, can be improved when implemented in practice.

One main goal of adding inks beyond CMYK is to extend color gamut, a desirable feature of color reproduction. The color gamut produced by CMYK inks (dashed line) is compared with to the extended color gamut (solid line) with the additional inks, Green and Orange, shown in Figure 7.

Generally a look-up table cannot utilize the whole color gamut because of its regular shape and some small parts are lost in the corners. If selected seed samples are not at the boundary of the color gamut for the cells at the edge, the color gamut of the look-up table based on these seed samples would be further decreased. Therefore, seed samples for the cells on the edge of the gamut should be selected as close as possible to the gamut boundary. To this end, the chroma (C^*_{ab}) metric was used as one of the selection criteria for the cells on the edge. The calculation equation for chroma is shown in Eq. (3)

$$C^*_{ab} = \sqrt{a^{*2} + b^{*2}}. \quad (3)$$

As described in the algorithm section, the initial seed sample set was updated for smoothness. A Gaussian function was used to smooth the initial seed sample set and a smoothed virtual sample set created. The distances between candidate samples and smoothed virtual samples in each cell

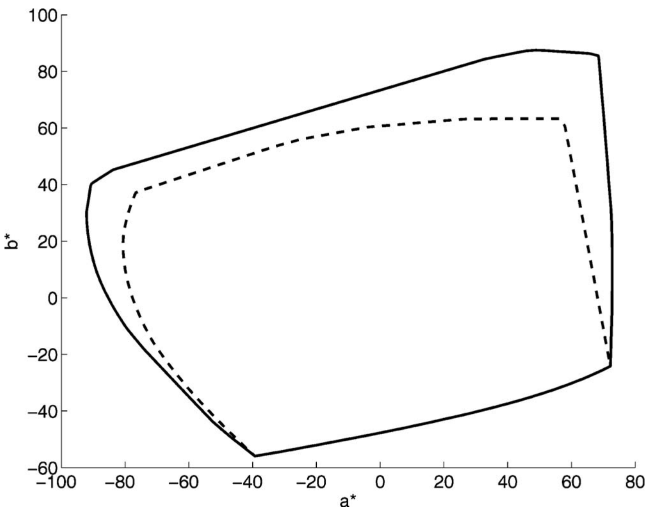

Figure 7. Gamut comparison between the CMYK ink set (dashed line) and the CMYKGO ink set (solid line) on the a*b* slice with L*=55.

were calculated and taken as a smoothness index, SI, shown in the following equation where ac represents area coverage

$$\mathrm{SI} = \sqrt{\sum_{i=1}^{6} (ac_{i,orig} - ac_{i,\mathrm{smooth}})^2}. \quad (4)$$

EXPERIMENTAL

The algorithm was tested using an Epson printer Pro 5500 to create color profiles optimized for the perceptual metrics. The experimental environmental temperature was controlled from 22 to 24°C. Epson's proprietary halftoning algorithm was used. Each color plane had 8 bit addressability, i.e., 256 levels ($2^8=256$). The method of changing drop size with increasing signal value was also proprietary. The amount of ink printed on the paper was controlled by creating six-plane, colored images. All samples were printed on Epson photo quality ink jet glossy paper, model number KA3N20MDK. Printed samples were dried for 1 h before measurement to ensure colors reached equilibrium. Each printed page included a custom target to ensure print-to-print repeatability.

The spectral measurements were performed using a GretagMacbeth Spectroscan spectrophotometer, having a 4 mm aperture with a 45/0 annular geometry and a wavelength range from 380 to 730 nm in 10 nm intervals. Only data between 400 and 700 nm were used, and colorimetric values were calculated for illuminants D50 and F11 and the CIE 1931 2° standard observer.

As described above, the spectral CYNSN printer model was developed and a large amount of virtual samples produced. The color constancy index and graininess index of each sample were calculated. The CIELAB space was divided into 16×16×16 cells, and each sample was assigned to a cell based on its colorimetric values. In each cell, different samples representing different ink combinations all achieved nearly the same color. The selection criteria were limited to color gamut, color constancy, graininess, and smoothness of the look-up tables.

The initial selection criterion is shown in the following equation:

$$Q = -k_1 \frac{C^*_{ab}}{\max(C^*_{ab})} + k_2 \frac{CII}{\max(CII)} + k_3 \frac{GI}{\max(GI)}. \quad (5)$$

CII represents the color inconstancy index, GI the graininess index, and C^*_{ab} chroma. The parameters k_1, k_2, and k_3 were used to adjust the weight of each metric. The chroma factor has a negative sign so that quality is improved as the metric decreases in magnitude for all the metrics. In one implementation, the weighting coefficients, k_1, k_2, and k_3, were set to 4, 1, and 0.5, respectively, as shown in Eq. (6). The large weighting was applied to chroma because a large color gamut is desirable. Note that the chroma metric was only applied on the cells of the gamut boundary. Color inconstancy was weighted twice the magnitude of graininess. In this implementation, CII was deemed the main contributor of image quality. Furthermore, it was recognized that the graininess index had limited accuracy because the halftoning was unknown.

$$Q = -4 * \frac{C^*_{ab}}{\max(C^*_{ab})} + \frac{CII}{\max(CII)} + 0.5 * \frac{GI}{\max(GI)}. \quad (6)$$

A sample with the minimal Q value was selected in each cell according to Eq. (6). As these selected samples distributed in CIELAB space irregularly, a three-dimensional, nonuniform interpolation algorithm is used to create a uniformly spaced 64×64×64 CLUT for each color plane. To perform the interpolation, the Matlab® function, "*griddata*" that uses Delaunay triangulation,[20,21] was used.

However, the look-up table based on the initial selected samples was not smooth, as shown in Figure 8, and area coverage fluctuations were observed. A large amount of candidate samples can decrease the fluctuations but cannot erase all of the fluctuations, so a smoothing program was developed as described in the perceptual metrics section.

The final look-up table was a trade-off between larger gamut, look-up table smoothness, color constancy, and graininess. With the addition of smoothness, the selection criterion was defined by Eq. (7)

$$Q = -k_1 \frac{C^*_{ab}}{\max(C^*_{ab})} + k_2 \frac{CII}{\max(CII)} + k_3 \frac{GI}{\max(GI)} + k_4 \frac{SI}{\max(SI)}, \quad (7)$$

where SI represents the smoothness index of the look-up table, and k_1, k_2, k_3, and k_4 were set to 2, 1, 0.5, and 1, respectively.

The look-up table created by the selected samples with the addition of smoothness index is plotted in Figure 9. Comparing Figs. 8 and 9, it is possible to see that the smoothness of the look-up table was improved significantly, though small fluctuations still can be detected.

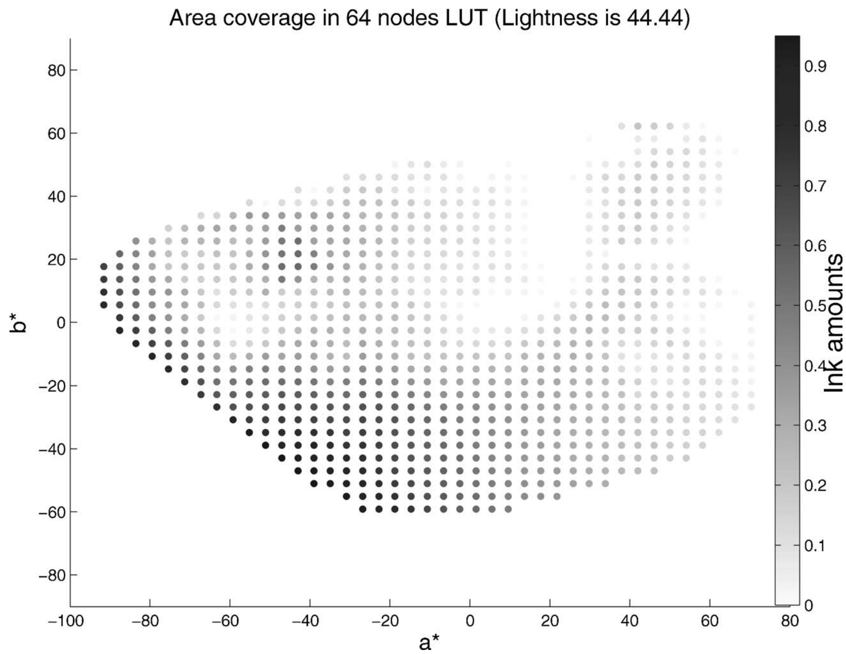

Figure 8. The interpolated area coverage for cyan ink at $L^*=44$ without the smoothness application.

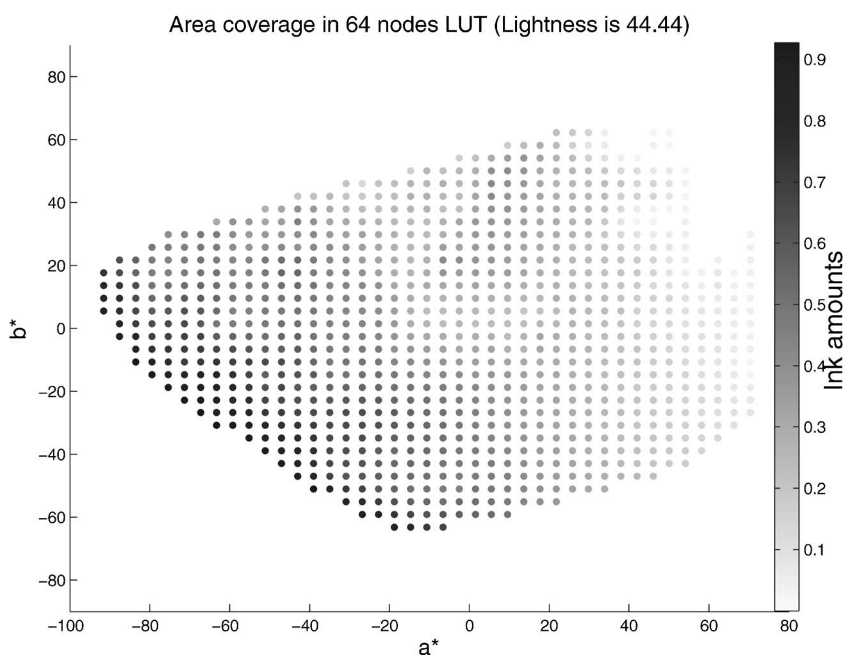

Figure 9. The interpolated area coverage for cyan ink at $L^*=44.0$ with smoothness applied.

In order to analyze the method thoroughly, three additional look-up tables were created according to different metrics for comparison to the above described six ink look-up table using all the metrics. They included two single metric look-up tables based on color inconstancy and graininess, and a four-ink look-up table without the green and orange inks using all of the metrics. The selection metrics for these three look-up tables are shown in the following equations:

1) Look-up table with minimum color inconstancy index

$$Q = \frac{CII}{\max(CII)}, \tag{8}$$

2) Look-up table with minimum graininess

$$Q = \frac{GI}{\max(GI)}, \tag{9}$$

3) Four color (CMYK) look-up table with all metrics

Table II. Performance of look-up tables with different metrics.

Metrics	Six ink Combined CLUT	CII CLUT	GI CLUT	Four ink Combined CLUT
Mean CII	1.16	0.74	1.54	2.55
Mean ΔE_{00}	2.33	2.22	3.28	2.39
Mean GI	0.68	0.86	0.63	0.76
Mean RMS	1.6%	1.6%	1.8%	1.5%
Gamut volume (CIE94)	1.99×10^5	1.95×10^5	2.01×10^5	1.72×10^5

$$Q = -2 * \frac{C^*_{ab}}{\max(C^*_{ab})} + \frac{CII}{\max(CII)} + 0.5 * \frac{GI}{\max(GI)} + \frac{SI}{\max(SI)}. \tag{10}$$

RESULTS AND DISCUSSION

In order to quantitatively analyze the performance of these look-up tables, a verification target was created that included a 21 step gray scale, the GretagMacbeth ColorChecker Color Rendition Chart, and the GretagMacbeth ColorChecker DC. The CIELAB values were based on direct spectrophotometry. The verification target was printed with the different look-up tables created by the different metrics: the six ink combined metric (Eq. (7)), the CII metric (Eq. (8)), the GI metric (Eq. (9)), and the four ink combined metric (Eq. (10)). As a qualitative evaluation, several pictorial images were also printed that included portraits, nature, and color gradients. These were evaluated visually.

The four printed targets were measured, and the CII and GI were calculated using direct spectrophotometry and scanning, respectively. The color differences between the original and reproduction were also calculated using the CIEDE2000 equation for Illuminant D50 and the 2° standard observer. The spectral RMS difference between the measured and predicted samples by the CYNSN model was calculated to check the accuracy of the print model. The gamut volume was calculated in CIE94-corrected CIELAB space[12] because it is more perceptually uniform than CIELAB space. The results are shown in Table II.

The results in Table II indicate that the CII metric look-up table (CII CLUT) provided the best color constancy (mean CII=0.74), the graininess metric look-up table (GI CLUT) provided the minimum graininess (mean GI=0.63), and the six ink look-up tables, including six ink combined CLUT, CII CLUT, and GI CLUT, increased color gamut volume about 16% compared with the four ink look-up table.

Comparing actual image prints under different light sources in a light booth, the prints created by the CII metric LUT had more stable colors than other prints, however, graininess was observed. The graininess metric LUT created smoother prints but their colors varied under different light sources. Overall, the six ink combined look-up table provided the best performance. This visual observation supported the quantitative results listed in Table II.

Table III. Statistical CII of four-ink samples and six-ink samples in the same four-ink gamut.

	Minimum CII	Average CII	95th Percentile CII	Maximum CII
Four-ink sample group	0.008	3.23	10.54	14.40
Six-ink sample group	0.004	2.32	8.12	14.82

Based on evaluating each ink plane of these look-up tables, the CII metric look-up table used more black ink whereas the graininess metric look-up table combined more chromatic inks, as expected. Black inks generally provide relatively flat spectral properties in prints which tend to achieve higher color constancy, yet increase graininess. On the other hand, the samples composed by chromatic inks tend to have jagged spectral curves causing larger color inconstancy. These tendencies, however, are a simplification. For detail on the relationship between the spectral reflectance and color constancy, see Ref. 22.

Color reproduction accuracy was primarily a function of errors in the printer model and interpolation, and secondarily measurement uncertainty and print variability. The accuracy differences among these look-up tables were mainly caused by errors of the printer model rather than interpolation because they used the same interpolation technique. Generally the printer model had relatively higher accuracy for samples with larger black ink components because of low prediction errors from spectrally flat black inks. Therefore, the CII metric look-up table achieved relatively higher color reproduction accuracy than the graininess metric look-up table.

The four-ink look-up table could not provide good performance because it did not include green and orange inks. In order to further analyze the advantages provided by these additional inks, the color inconstancy indices of samples composed of four inks, CMYK, were compared with that of the samples composed of six inks, CMYKGO, within the intersection of the two color gamuts, that is, the CMYK gamut. That is, the samples in the extended gamut were omitted. The CII statistics for these two groups of samples are shown in Table III. It clearly indicates that the additional inks not only extended color gamut but also provided more potential to improve perceptual image quality.

CONCLUSIONS

An algorithm was developed to deal with the one-to-many mapping problem when building color look-up tables for multi-ink printing. The unique feature of the algorithm is the combination of color constancy and the graininess as selection criteria among ink combinations yielding a similar color. The algorithm was tested with several targets and demonstrated improvements in perceptual image quality. Furthermore, one can imagine a number of criteria that can be used as selection metrics, individually or combined, such as ink amount, sharpness, maximum black ink amount, and print precision. A theoretical analysis is also warranted to understand the interrelationships between the number of inks, their spectral properties, color constancy, and color gamut.

ACKNOWLEDGMENTS

This research was sponsored by the Seiko Epson Corporation. Their financial support, equipment and consumables donations, and software and technical support are sincerely appreciated. We also would like to thank Mr. Rod Heckaman for editorial assistance.

REFERENCES

[1] J. A. C. Yule, *Principles of Color Reproduction* (Wiley, New York, 1967).
[2] M. R. Rosen, E. F. Hattenberger, and N. Ohta, J. Imaging Sci. Technol. **48**, 228–232 (2004).
[3] H. Kueppers, "Printing process where each incremental area is divided into a chromatic area and an achromatic area and wherein the achromatic areas are printed in black and white and the chromatic areas are printed in color sub-sections", US Patent No. 4,812,899 (1989).
[4] V. Ostromoukhov, "Chromaticity gamut enhancement by heptatone multi-color printing", Proc. SPIE **1909**, 139–151 (1993).
[5] R. Balasubramanian, "System for printing color images with extra colorant in addition to primary colorants", US Patent No. 5,870,530 (1999).
[6] H. Boll, "A color to colorant transformation for a seven ink process", Proc. SPIE **2170**, 108–118 (1994).
[7] E. N. Dalal, R. Balasubramanian, and R. V. Klassen, "System for printing color images with extra colorants in addition to primary colorants", US Patent No. 5,892,891 (1999).
[8] Y. Chen, R. S. Berns, and L. A. Taplin, "Six color printer characterization using an optimized cellular Yule-Nielsen spectral Neugebauer model", J. Imaging Sci. Technol. **48**, 519–528 (2004).
[9] L. A. Taplin and R. S. Berns, "Spectral color reproduction based on a six-color ink jet output system", *Proc. IS&T/SID Ninth Color Imaging Conference* (IS&T, Springfield, VA, 2001) pp. 209–213.
[10] R. S. Berns, *Billmeyer and Saltzman's Principles of Color Technology*, 3rd ed. (Wiley, New York, 2000).
[11] H. S. Fairman, "Metameric correction using parametric decomposition", Color Res. Appl. **16**, 337–341 (1987).
[12] Y. Chen, R. S. Berns, L. A. Taplin, and F. H. Imai, "A multi-ink color-separation algorithm maximizing color constancy", *Proc. IS&T/SID Eleventh Color Imaging Conference* (IS&T, Springfield, VA, 2003) pp. 277–281.
[13] R. S. Berns and F. W. Billmeyer, "Proposed indices of metamerism with constant chromatic adaptation", Color Res. Appl. **8**, 186–189 (1983).
[14] M. R. Luo and R. W. G. Hunt, "A chromatic adaptation transform and a colour inconstancy index", Color Res. Appl. **23**, 154–158 (1998).
[15] International Commission on Illumination, CIE Pub 159: 2004. *A Color Appearance Model for Color Management Systems* (CIE Central Bureau, Vienna, 2004).
[16] R. P. Dooley and R. Shaw, "Noise perception in electrophotography", J. Appl. Photogr. Eng. **5**, 190–196 (1979).
[17] M. Hino, K. Kagitani, M. Kojima, and S. Imakawa, "A new method for the graininess evaluation", *Proc. IS&T's NIP11: International Congress on Advances in Non-Impact Printing* (IS&T, Springfield, VA, 1995) pp. 489–492.
[18] X. M. Zhang and B. A. Wandell, "A spatial extension to CIELAB for digital color image reproduction", SID Symp. Tech. Digest **27**, 731–734 (1996).
[19] G. M. Johnson and M. D. Fairchild, "A top down description of S-CIELAB and CIEDE2000", Color Res. Appl. **28**, 425–435 (2003).
[20] C. B. Barber, D. P. Dobkin, and H. T. Huhdanpaa, "The Quickhull Algorithm for Convex Hulls", ACM Trans. Math. Softw. **22**, 469–483 (1996). Available in HTML format at http://www.acm.org/pubs/citations/journals/toms/1996-22-4/p469-barber/ and in PostScript format at ftp://geom.umn.edu/pub/software/qhull-96.ps
[21] National Science and Technology Research Center for Computation and Visualization of Geometric Structures (The Geometry Center, University of Minnesota, 1993).
[22] R. S. Berns, F. W. Billmeyer, Jr., and R. S. Sacher, "Methods for generating spectral reflectance functions leading to color-constant properties", Color Res. Appl. **10**, 73–83 (1985).